Electronic Supplementary Information

Copper-based metal-organic framework for sensitive sensing of $Cr_2O_7^{2-}$ in aqueous solution

Qiuxiang Feng,[a] Linghan Shi[b], Jiatong Dai,[a] Qifan Jiang,[a] Feng Cao,[a] Qianli Zhang,[a] Wei Chen,[*, b] Jie Liu,[*, a]

[a] School of Chemistry and Life Sciences, Suzhou University of Science and Technology, Suzhou, Jiangsu 215009, P.R. China.

[b] School of Nuclear Science and Technology, National Synchrotron Radiation Laboratory, State Key Laboratory of Advanced Glass Materials, Anhui Provincial Engineering Research Center for Advanced Functional Polymer Films, University of Science and Technology of China, Hefei, Anhui 230029, P.R. China.

E-mail: wc003@ustc.edu.cn

jliu@mail.usts.edu.cn

Materials

All chemicals were used as received without further purification. Copper(II) acetate monohydrate ($Cu(CH_3COO)_2 \cdot H_2O$, 2,5-dihydroxyterephthalic acid (DHTA), and ethanol (EtOH) were obtained from Shanghai Aladdin Biochemical Technology Co., Ltd. Potassium carbonate (K_2CO_3), calcium chloride ($CaCl_2$), and magnesium chloride ($MgCl_2$) were purchased from Shanghai Meril Chemical Technology Co., Ltd. N, N-dimethylformamide (DMF) and sodium hydroxide (NaOH) were acquired from Beijing Bailingwei Technology Co., Ltd. All reagents were of analytical grade (AR), and all solutions were prepared using deionized distilled water (DDW).

General procedures

The synthesized materials were comprehensively characterized using multiple analytical techniques. The crystal structure of the target material was characterized by X-ray diffraction (XRD, Ultima IV, Rigaku, Japan) under operating conditions of 40 kV and 40 mA, with a 2θ scanning range from 5° to 40° at a rate of 0.2°/min. The morphological features of the samples were examined using a field emission scanning electron microscope (SEM, S4800, Hitachi, Japan). Fourier transform infrared spectra were acquired on a Spectrum Two spectrometer (FT-IR, PerkinElmer, USA) in the wavenumber range of 500-4000 cm^{-1}. Specific surface area and pore size distribution were determined using an automated surface area and porosity analyzer (ASAP 2020M, Micromeritics, USA). Prior to analysis, the material was dried at 100 °C for 12 h, followed by full pore structure analysis in a liquid nitrogen environment at 77 K. The elemental composition and chemical states were investigated by X-ray photoelectron spectroscopy (XPS, K-Alpha, Thermo Fisher Scientific), with charge calibration referenced to the C 1s peak at 284.8 eV. UV-Vis absorption measurements were performed with a UV spectrophotometer (HB-7, Beijing Haotianhui Instrument Co., China) using barium sulfate as a reference, with wavelength scanning from 200 to 800 nm. Thermal stability was evaluated via thermogravimetric analysis (TGA, Pyris 1, PerkinElmer, USA). The fluorescence properties of the material were tested using a fluorescence spectrophotometer (PL, Tianjin Port East Technology Co., Ltd. F-380), with the excitation wavelength set at 310 nanometers.

Experimental procedures.

Synthetic procedures of ligand (2,5-dimethoxyterephthalic acid)

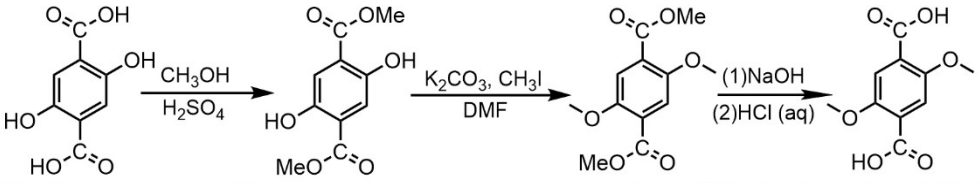

2,5-dihydroxybenzoic acid **a** **b** **2,5-dimethoxyterephthalic acid**

Scheme S1. The synthetic route for 2,5-dimethoxyterephthalic acid.

*Synthesis of 2,5-dihydroxybenzoic acid methyl ester **a***. 2,5-dihydroxybenzoic acid (2 g) was placed in a two-necked round-bottom flask equipped with a magnetic stir bar. The reaction vessel was subjected to three vacuum-nitrogen purge cycles before the addition of anhydrous methanol (60 mL) and concentrated sulfuric acid (0.5 mL) under continuous nitrogen flow. The rubber septum was subsequently replaced with a glass stopper, sealed with PTFE tape, and secured with a clamp. The reaction mixture was heated to 70 °C under reflux with constant stirring for 48 hours, with daily monitoring by thin-layer chromatography (TLC, dichloromethane as eluent). For TLC analysis, the flask was temporarily removed from the heat source, cooled to ambient temperature, and sampled under nitrogen atmosphere. Upon reaction completion (as determined by TLC), the system was cooled to room temperature and concentrated by rotary evaporation. The crude product was purified by aqueous workup, followed by vacuum drying at 70 °C to afford green needle-like crystals (product **a**) in 84.9% yield (969.7 mg). ^{1}H NMR (400 MHz, $CDCl_3$) δ 10.07 (s, 2H, ArOH), 7.47 (s, 2H, ArCH), 3.97 (s, 6H, CH_3) (Figure S1).

*Synthesis of 2,5-dimethoxyterephthalic acid methyl ester **b.*** 2,5-dihydroxybenzoic acid methyl ester **a** (200 mg) and potassium carbonate (550 mg) were placed in a round-bottom flask equipped with a magnetic stir bar. Then, 6 mL of N, N-dimethylformamide was added, and the mixture was thoroughly mixed before 1 mL of iodomethane was gradually added drop by drop. The reaction mixture was heated to 85 °C under reflux conditions with vigorous stirring for 24 hours, with reaction progress monitored by thin-layer chromatography (TLC). Upon completion, the mixture was centrifuged and the resulting solid was dried at 60 °C under vacuum. The crude product was purified by column chromatography using a gradient eluent system of dichloromethane/petroleum ether (v/v = [1:1]), yielding compound **b** as a white crystalline solid (184 mg, yield 81.9%).^{1}H NMR (600 MHz, $CDCl_3$) δ 7.40 (s, 2H, ArCH), 3.92 (s, 6H, CH_3), 3.89 (s, 6H, CH_3) (Figure S2).

Synthesis of 2,5-dimethoxyterephthalic acid. 2,5-dimethoxyterephthalic acid methyl ester **b** (130 mg) was placed in a round-bottom flask equipped with a magnetic stir bar. A 3 M NaOH solution in EtOH/H_2O (1:1 v/v, 4 mL) was added as the reaction solvent. The mixture was heated to 70 °C under reflux conditions with continuous stirring for 24 hours, with reaction progress monitored by thin-layer chromatography (TLC). Upon completion, the reaction was cooled to ambient temperature and acidified to pH≈2 by dropwise addition of concentrated HCl with vigorous stirring in an ice-water bath. The resulting suspension was concentrated by rotary evaporation, and the precipitate was collected by vacuum filtration. The crude product was washed repeatedly with distilled water until neutral pH was achieved, then dried under vacuum to afford white crystalline solid 2,5-dimethoxyterephthalic acid (100.8 mg, yield 87.1%).^{1}H NMR (600 MHz, DMSO-d_6) δ 7.30 (s, 2H, ArCH), 3.78 (s, 6H, CH_3) (Figure S3).

Preparation of Cu-OCH_3 MOF

The Cu-OCH_3 MOF was synthesized via solvothermal method. In a typical preparation, 2,5-dimethoxyterephthalic acid (30 mg) and copper(II) acetate monohydrate (($Cu(CH_3COO)_2 \cdot H_2O$, 35.94 mg) were combined with N,N-dimethylformamide (DMF, 3.6 mL) in an 8 mL glass vial. The sealed vessel was subjected to ultrasonic treatment for 20 min to ensure complete dissolution and homogenization of the reactants, followed by solvothermal reaction at 110 °C for 48 h. After cooling to room temperature, the resulting crystals were isolated by centrifugation (3000 rpm, 5 min) and washed sequentially with DMF (3×5 mL) and deionized water (3×5 mL) to remove unreacted species and residual solvent. The purified product was dried at 70 °C under vacuum for 12 h, yielding pale blue crystalline Cu-OCH_3 MOF (44.9 mg) (Scheme 1).

Stability test of Cu-OCH_3 MOF

The chemical stability of the Cu-OCH_3 MOF was assessed by exposing it to aqueous solutions of varying pH. Solutions (10 mL) with pH values of 1.0, 3.0, 5.0, 9.0, 11.0 and 13.0 were prepared using hydrochloric acid or sodium hydroxide as required. Aliquots (10 mg) of the MOF were then immersed in 5 mL of each pH solution and at room temperature for 24 hours. Subsequently, the solid products were recovered by filtration, copiously washed with deionized water, and dried at 70 °C for 12 hours prior to PXRD characterization.

Fluorescence quenching experiments

In the standard fluorescence quenching experiment procedure, a certain volume and concentration of quenching catalyst will be added to a solution of known volume and concentration of chromate ions ($Cr_2O_7^{2-}$). After mixing evenly, the fluorescence spectrum will be recorded immediately using the F-380 fluorescence spectrometer (λ_{ex}=310 nm). The subsequent experiments systematically investigated key parameters, including the ion selectivity experiment, anti-interference experiment, sensitivity detection experiment and mechanism exploration experiment.

Ion-selective experiment. Comprehensive ion selectivity study was conducted by preparing aqueous solutions (10^{-3} M) of various anions and cations. Anion solutions were prepared from sodium salts (NaCl, Na_2CO_3, $NaHCO_3$, $NaNO_2$, $Na_2C_2O_4$, Na_2SO_4, NaH_2PO_4, NaAc, $Na_2S_2O_3$, NaClO and $K_2Cr_2O_7$), while cation solutions were derived from chloride salts ($AlCl_3$, $BaCl_2$, KCl, $CdCl_2$, CuCl, $CuCl_2$, $CrCl_2$, $MgCl_2$, $NiCl_2$, $SnCl_2$, $CaCl_2$, NaCl and $CoCl_2$). All solutions were freshly prepared in deionized water immediately before use. For fluorescence measurements, Cu-OCH_3 MOF (2 mg) was dispersed in deionized water (40 mL) via ultrasonication for 30 min to obtain a homogeneous suspension. Aliquots (0.5 mL) of the MOF dispersion were combined with 2 mL of each ion solution in glass vials and vigorously mixed after, fluorescence spectra were recorded using an F-380 spectrofluorometer (λ_{ex}=310 nm) with deionized water serving as the blank control.

Anti-interference experiment. In order to study the anti-interference performance of fluorescence detection, four distinct mixed ion systems were prepared: (a) an equimolar anion mixture (Cl^-, CO_3^{2-}, HCO_3^-, NO_2^-, $C_2O_4^{2-}$, SO_4^{2-}, $H_2PO_4^-$, Ac^-, $S_2O_3^{2-}$, ClO^- and $Cr_2O_7^{2-}$) with each anion at 10^{-3} M, (b) the same anion mixture with total concentration of 11×10^{-3} M (11-fold excess relative to $Cr_2O_7^{2-}$), (c) an equimolar cation mixture (Al^{3+}, Ba^{2+}, K^+, Cd^{2+}, Cu^+, Cu^{2+}, Cr^{2+}, Mg^{2+}, Ni^+, Sn^{2+}, Ca^{2+}, Na^+, Co^{2+}) at 10^{-3} M each and (d) the same cation mixture with total concentration of 14×10^{-3} M (14-fold excess relative to $Cr_2O_7^{2-}$). For each test, 0.5 mL of the ultrasonically dispersed Cu-OCH_3 MOF suspension was combined with 2 mL of the respective ion mixture and vortex-mixed. Fluorescence spectra were immediately acquired using an F-380 spectrofluorometer (λ_{ex}=310 nm) following 30 s of equilibration.

Sensitivity detection experiment. The detection sensitivity of Cu-OCH_3 MOF toward $Cr_2O_7^{2-}$ was evaluated by preparing a concentration gradient spanning from 10^{-5} to 10^{-3} M (specifically: 1, 2, 3, 4, 5, 6, 7, 8, 9×10^{-5} M and 1, 2, 3, 4, 5, 6, 7, 8, 9×10^{-4} M, culminating at 10^{-3} M). For each measurement, 0.5 mL of the uniformly dispersed Cu-OCH_3 MOF suspension was combined with 2 mL of the corresponding $Cr_2O_7^{2-}$ solution. After thorough mixing at ambient temperature (25±1°C), fluorescence spectra were immediately recorded using an F-380 spectrofluorometer (λ_{ex}=310 nm).

Cycle Experiment. To evaluate the cyclic stability of Cu-OCH_3 MOF, 20 mg of the Cu-OCH_3 MOF material was added to 2 mL of a 10^{-2} M $Cr_2O_7^{2-}$ solution and stirred for 5 min. After centrifugation, the supernatant was removed. Deionized water was then added, and the mixture was sonicated for 5 min, followed by centrifugation and removal of the clear liquid. This washing procedure was repeated six times to eliminate residual $Cr_2O_7^{2-}$. The solid powder was dried in an electric heating oven at 70 °C. The entire process was then repeated to obtain Cu-OCH_3 MOF materials that had undergone 2 and 3 cycles.

A 2 mg portion of each cycled Cu-OCH_3 MOF sample was dispersed in 40 mL of deionized water via sonication for 30 min to achieve a uniform dispersion. Then, 500 μL of the dispersion was transferred into a small glass vial, mixed with 2 mL of a freshly prepared 10^{-3} M $Cr_2O_7^{2-}$ solution, and shaken thoroughly. Deionized water was used as a blank reference. The samples were incubated in a constant-temperature shaker for 30 min, after which their fluorescence intensities (λ_{ex}=310 nm) were measured using an F-380 steady-state/transient fluorescence spectrometer, both in deionized water and in the $Cr_2O_7^{2-}$ solution.

Mechanism exploration experiment. To elucidate the mechanism of fluorescence quenching, a series of characterization techniques were employed. X-ray diffraction (XRD) was used to assess the potential degradation of the MOF framework in anionic solutions. Fourier-transform infrared (FT-IR) spectroscopy and X-ray photoelectron spectroscopy (XPS) were applied to probe the interactions between anions and the MOF. Cyclic voltammetry (CV) was conducted to investigate the possibility of a redox reaction, Ultraviolet-visible (UV-Vis) absorption spectra and PL excitation spectra of the MOF materials were analyzed to check for the presence of competitive excitation absorption. Fluorescence lifetime and ultraviolet-visible (UV-Vis) absorption spectra were analyzed along with the PL emission spectra of the MOF materials to check for the presence of dynamic quenching processes.

The sample for XRD, FT-IR and XPS analyses was prepared by immersing 30 mg of the Cu-OCH_3 MOF in a $Cr_2O_7^{2-}$ solution for 24 hours prior to measurement. For the cyclic voltammetry (CV) tests, a 20 mL saturated KCl solution served as the electrolyte. CV scans were performed on the following sequentially prepared systems: the pure electrolyte, a mixture of 10 mL of 10^{-3} M $Cr_2O_7^{2-}$ solution with 10 mL of saturated KCl, 1.4 mg of the MOF dispersed in 20 mL of saturated KCl and a mixture where 1.4 mg of the MOF was first combined with 10 mL of 10^{-3} M $Cr_2O_7^{2-}$ solution, allowed to stand for 30 minutes, and then mixed with 10 mL of saturated KCl. Furthermore, ultraviolet-visible (UV-Vis) absorption spectra were acquired for a series of cation and anion solutions (including Al^{3+}, Ba^{2+}, K^+, Cd^{2+}, Cu^+, Cu^{2+}, Cr^{2+}, Mg^{2+}, Ni^+, Sn^{2+}, Ca^{2+}, Na^+, Co^{2+},Cl^-, CO_3^{2-}, HCO_3^-, NO_2^-, $C_2O_4^{2-}$, SO_4^{2-}, $H_2PO_4^-$, Ac^-, $S_2O_3^{2-}$, Cl^- and $Cr_2O_7^{2-}$, all at

10^{-3} M) and a Cu-OCH_3 MOF dispersion, using a HB-7 spectrophotometer over the wavelength range of 200 to 800 nm. The emission spectrum and excitation spectrum of the Cu-OCH_3 MOF material were recorded using the F-380 fluorescence spectrometer (λ_{ex}=310 nm). The fluorescence lifetime of the Cu-OCH_3 MOF material was measured using the Edinburgh FLS1000 (λ_{ex}=310 nm, λ_{em}=393 nm).

Figures.

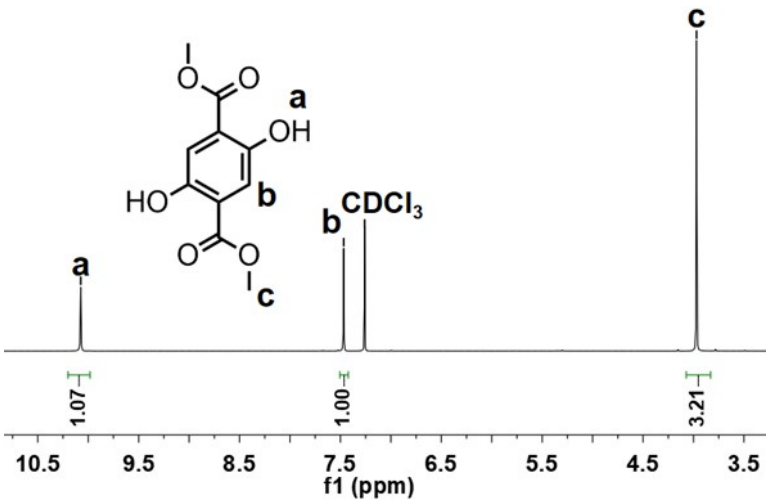

Figure S1. [1]H-NMR spectrum of 2,5-dihydroxybenzoic acid methyl ester.

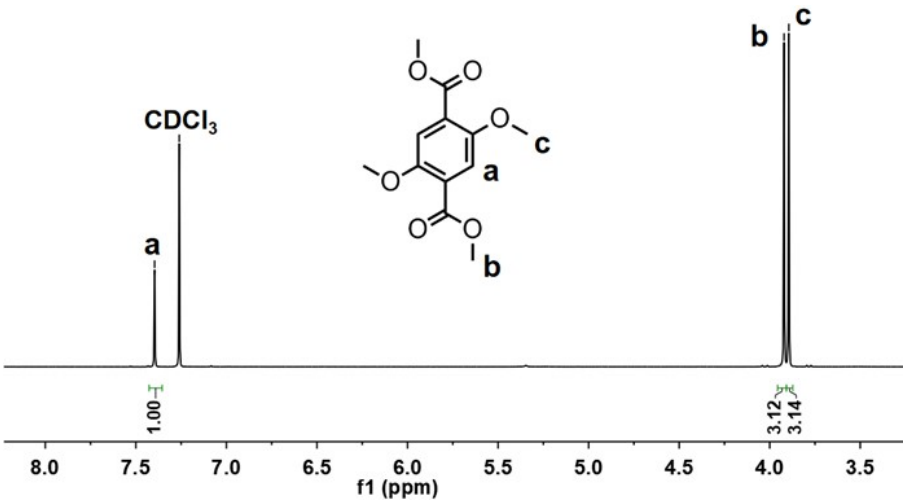

Figure S2. [1]H-NMR spectrum of 2,5-dimethoxyterephthalic acid methyl ester.

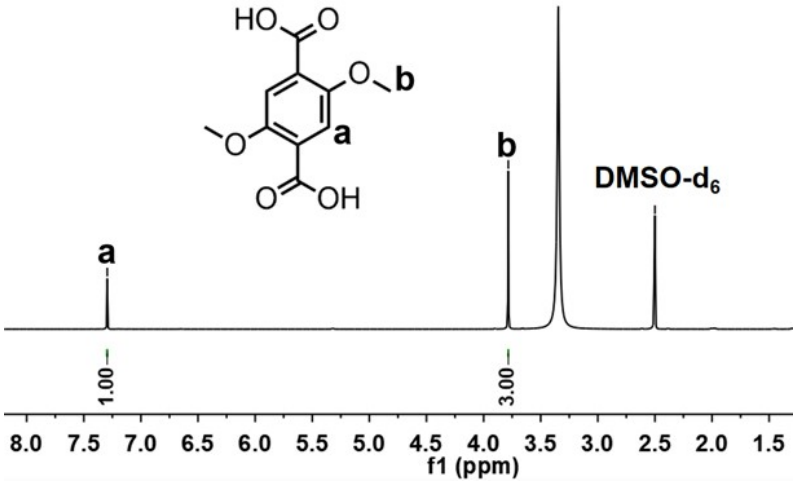

Figure S3. ^{1}H-NMR spectrum of 2,5-dimethoxyterephthalic acid.

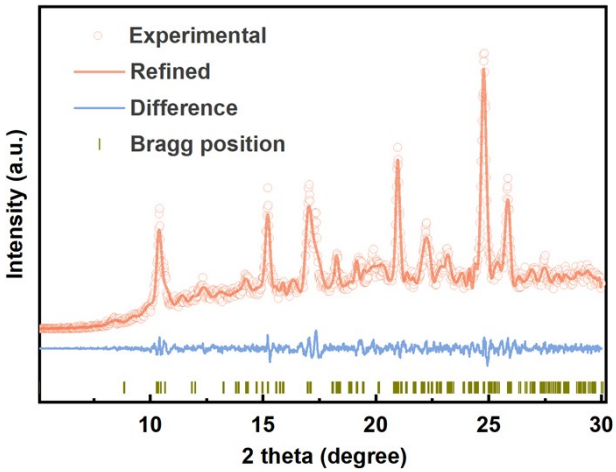

Figure S4. Pawley refinement of the experimental diffraction pattern of an as-made sample of Cu-OCH_3 MOF. The experimental PXRD pattern (orange hollow circle), the refined curve (orange line), the difference plot (blue line) and the allowed peak positions (green ticks). The values of R_{wp} and R_p are 10.65% and 8.73%, respectively.

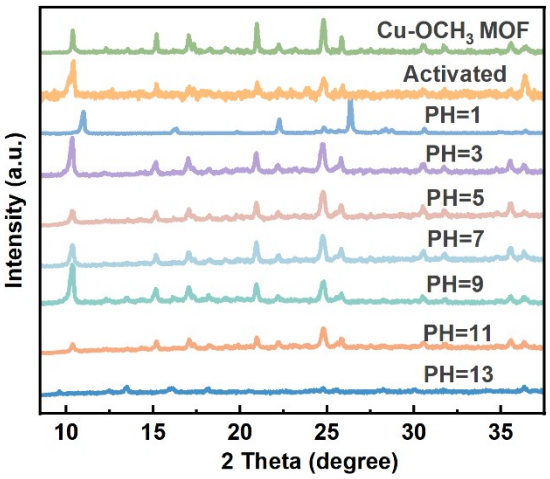

Figure S5. PXRD patterns of Cu-OCH_3 MOF samples at different pH values and after activation treatment.

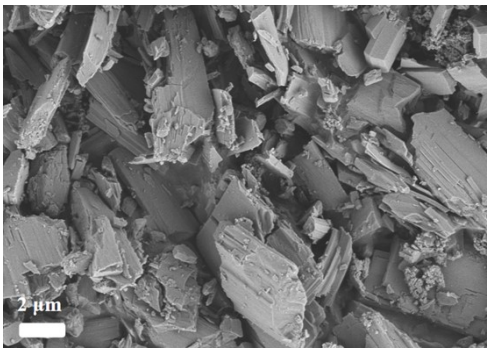

Figure S6. Scanning electron microscope image of Cu-OCH_3 MOF.

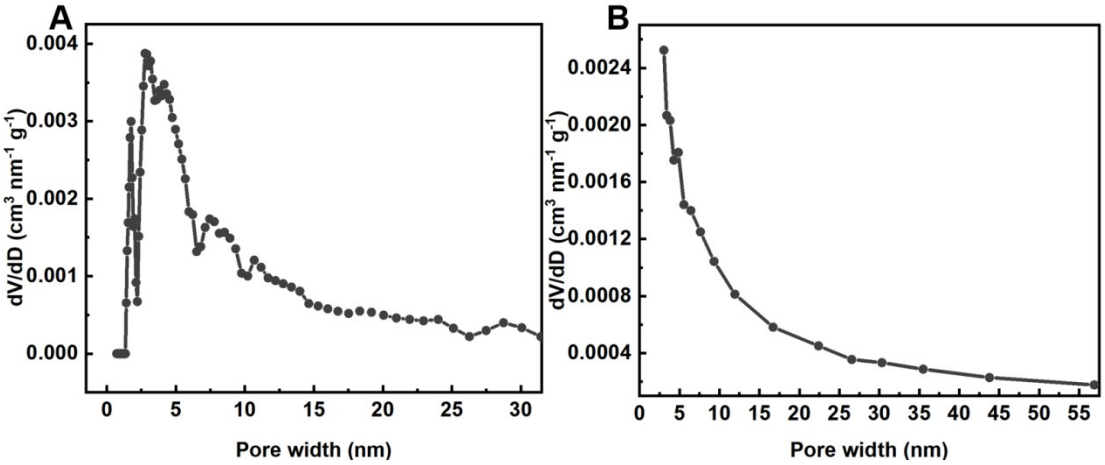

Figure S7. Pore size distribution of Cu-OCH_3 MOF with density functional theory (DFT) (A) and (B) Barrett-Joyner-Halenda (BJH) theory.

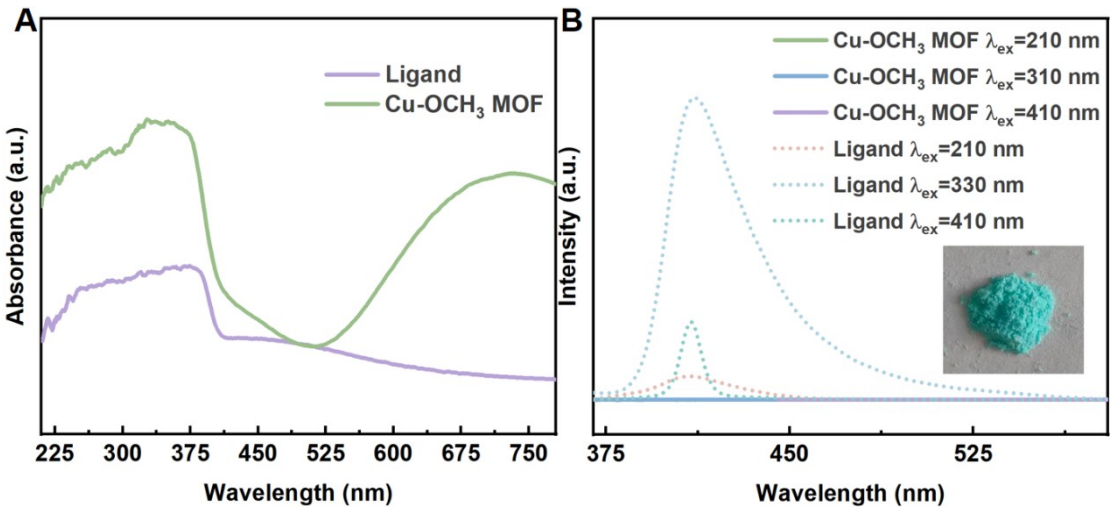

Figure S8. (A) Solid UV-Vis spectra and (B) Solid emission spectra of Cu-OCH_3 MOF and 2,5-dimethoxyterephthalic acid ligand. Inset: photograph of Cu-OCH_3 MOF sample.

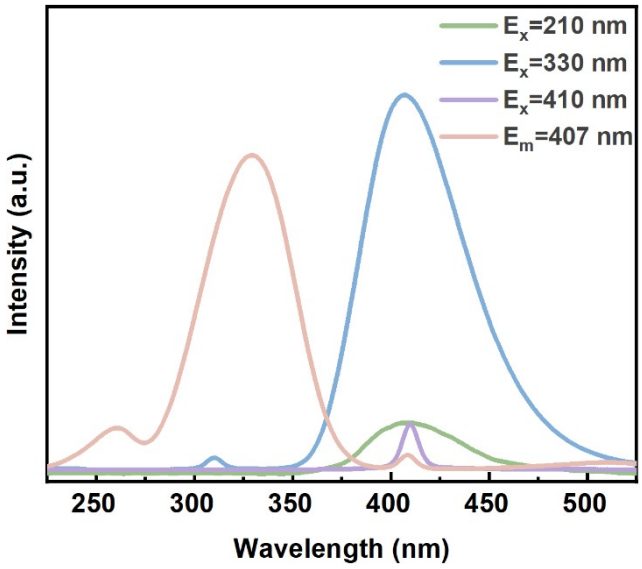

Figure S9. Photoluminescence spectra of the ligand in aqueous solution.

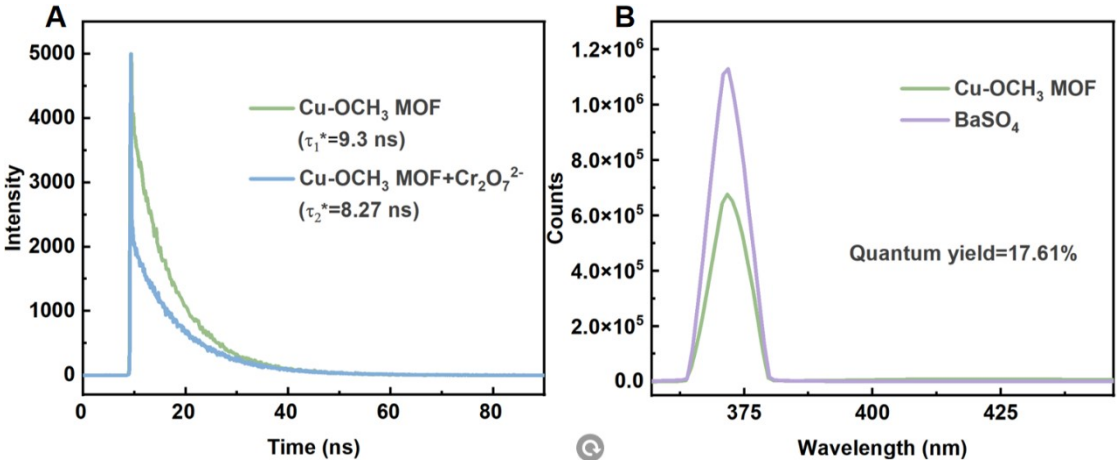

Figure S10. (A) Time-resolved fluorescence decay curves of Cu-OCH_3 MOF (τ_1*=9.3 ns) and Cu-OCH_3 MOF+$Cr_2O_7^{2-}$ (τ_2*=8.27 ns), (B) Quantum yield of Cu-OCH_3 MOF in water (quantum yield: 17.61%).

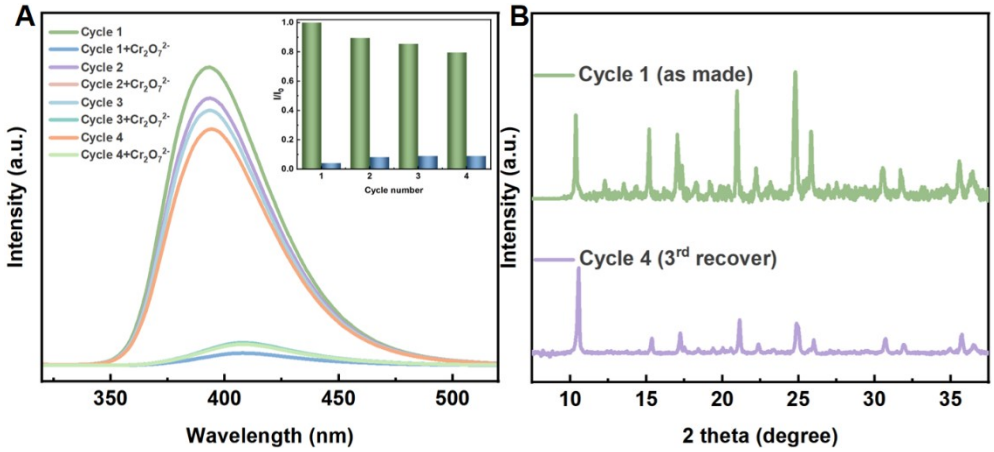

Figure S11. (A) Fluorescence spectra of Cu-OCH_3 MOF for $Cr_2O_7^{2-}$ sensing across multiple fabrication and recovery cycles. (B) PXRD patterns of as made Cu-OCH_3 MOF (green line) and recovered Cu-OCH_3 MOF (purple line) after cycle experiment of $Cr_2O_7^{2-}$ sensing.

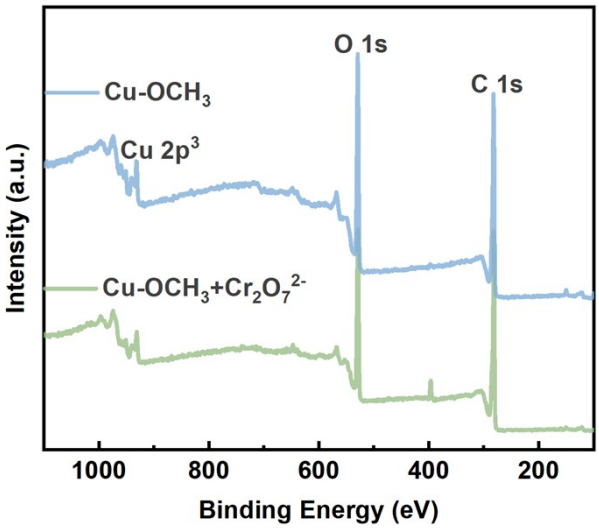

Figure S12. (A) XPS spectra before and after Cu-OCH_3 MOF immersion in $Cr_2O_7^{2-}$ (10^{-3} M).

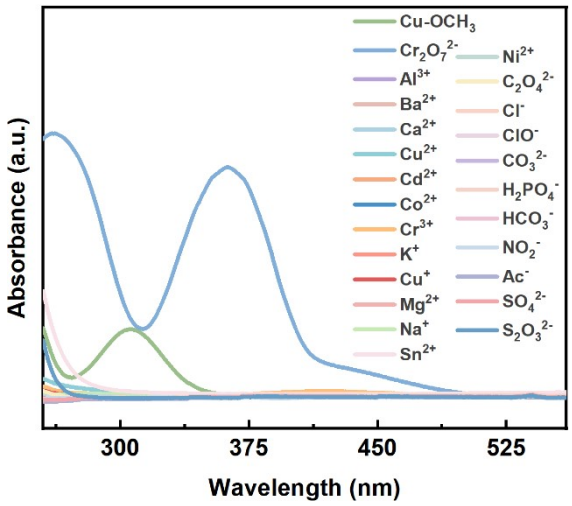

Figure S13. UV-Vis spectra of Cu-OCH_3 MOF, $Cr_2O_7^{2-}$ and other relevant anions and cations.

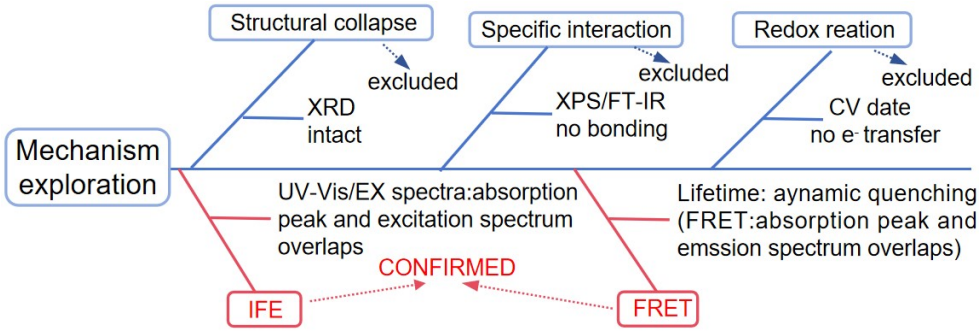

Scheme S2. Exploration progress for the detection mechanism of Cu-OCH_3 MOF towards $Cr_2O_7^{2-}$.

Table S1. Atomic coordinates of the ABC-stacking mode of Cu-OCH_3 MOF.

Space group: *R*-3

a=12.26 Å, *b*=16.24 Å, and *c*=8.02 Å

α =90°, β = 126°, and γ = 89°

residual factors: R_p=8.73%, R_{wp}=10.65%

atomic	X	Y	Z
C1	0.90093	0.12657	0.30708
C2	0.82199	0.18992	0.1468
C3	0.84129	0.20071	0.00192
C4	0.77105	0.2602	0.85658
C5	0.33502	0.04541	0.503
C6	0.50153	0.1234	0.43178
C7	0.34402	0.04611	0.22004
H8	0.91592	0.16096	0.99654
O9	0.79363	0.27373	0.71657
N10	0.37371	0.09116	0.39103
O11	0.98497	0.0807	0.28209
O12	0.81688	0.07526	0.31994
H13	0.35272	0.07587	0.6419
H14	0.50231	0.1825	0.36119
H15	0.238	0.06172	0.08459
C16	0.85647	0.20972	0.68774
H17	0.96675	0.15899	0.45755
H18	0.83341	0.21393	0.53094
H19	0.81667	0.15016	0.70369
H20	0.97036	0.21307	0.80518
C21	0.40093	0.62657	0.30708
C22	0.32199	0.68992	0.1468
C23	0.34129	0.70071	0.00192
C24	0.27105	0.7602	0.85658
C25	0.83502	0.54541	0.503
C26	0.00153	0.6234	0.43178
C27	0.84402	0.54611	0.22004
H28	0.41592	0.66096	0.99654
O29	0.29363	0.77373	0.71657
N30	0.87371	0.59116	0.39103
O31	0.48497	0.5807	0.28209
O32	0.31688	0.57526	0.31994
H33	0.85272	0.57587	0.6419
H34	0.00231	0.6825	0.36119
H35	0.738	0.56172	0.08459
C36	0.35647	0.70972	0.68774
H37	0.46675	0.65899	0.45755

H38	0.33341	0.71393	0.53094
H39	0.31667	0.65016	0.70369
H40	0.47036	0.71307	0.80518
C41	0.09907	0.12657	0.69292
C42	0.17801	0.18992	0.8532
C43	0.15871	0.20071	0.99808
C44	0.22895	0.2602	0.14342
C45	0.66498	0.04541	0.497
C46	0.49847	0.1234	0.56822
C47	0.65598	0.04611	0.77996
H48	0.08408	0.16096	0.00346
O49	0.20637	0.27373	0.28343
N50	0.62629	0.09116	0.60897
O51	0.01503	0.0807	0.71791
O52	0.18312	0.07526	0.68006
H53	0.64728	0.07587	0.3581
H54	0.49769	0.1825	0.63881
H55	0.762	0.06172	0.91541
C56	0.14353	0.20972	0.31226
H57	0.03325	0.15899	0.54245
H58	0.16659	0.21393	0.46906
H59	0.18333	0.15016	0.29631
H60	0.02964	0.21307	0.19482
C61	0.59907	0.62657	0.69292
C62	0.67801	0.68992	0.8532
C63	0.65871	0.70071	0.99808
C64	0.72895	0.7602	0.14342
C65	0.16498	0.54541	0.497
C66	0.99847	0.6234	0.56822
C67	0.15598	0.54611	0.77996
H68	0.58408	0.66096	0.00346
O69	0.70637	0.77373	0.28343
N70	0.12629	0.59116	0.60897
O71	0.51503	0.5807	0.71791
O72	0.68312	0.57526	0.68006
H73	0.14728	0.57587	0.3581
H74	0.99769	0.6825	0.63881
H75	0.262	0.56172	0.91541
C76	0.64353	0.70972	0.31226
H77	0.53325	0.65899	0.54245
H78	0.66659	0.71393	0.46906
H79	0.68333	0.65016	0.29631
H80	0.52964	0.71307	0.19482
C81	0.09907	0.87343	0.69292

C82	0.17801	0.81008	0.8532
C83	0.15871	0.79929	0.99808
C84	0.22895	0.7398	0.14342
C85	0.66498	0.95459	0.497
C86	0.49847	0.8766	0.56822
C87	0.65598	0.95389	0.77996
H88	0.08408	0.83904	0.00346
O89	0.20637	0.72627	0.28343
N90	0.62629	0.90884	0.60897
O91	0.01503	0.9193	0.71791
O92	0.18312	0.92474	0.68006
H93	0.64728	0.92413	0.3581
H94	0.49769	0.8175	0.63881
H95	0.762	0.93828	0.91541
C96	0.14353	0.79028	0.31226
H97	0.03325	0.84101	0.54245
H98	0.16659	0.78607	0.46906
H99	0.18333	0.84984	0.29631
H100	0.02964	0.78693	0.19482
C101	0.59907	0.37343	0.69292
C102	0.67801	0.31008	0.8532
C103	0.65871	0.29929	0.99808
C104	0.72895	0.2398	0.14342
C105	0.16498	0.45459	0.497
C106	0.99847	0.3766	0.56822
C107	0.15598	0.45389	0.77996
H108	0.58408	0.33904	0.00346
O109	0.70637	0.22627	0.28343
N110	0.12629	0.40884	0.60897
O111	0.51503	0.4193	0.71791
O112	0.68312	0.42474	0.68006
H113	0.14728	0.42413	0.3581
H114	0.99769	0.3175	0.63881
H115	0.262	0.43828	0.91541
C116	0.64353	0.29028	0.31226
H117	0.53325	0.34101	0.54245
H118	0.66659	0.28607	0.46906
H119	0.68333	0.34984	0.29631
H120	0.52964	0.28693	0.19482
C121	0.90093	0.87343	0.30708
C122	0.82199	0.81008	0.1468
C123	0.84129	0.79929	0.00192
C124	0.77105	0.7398	0.85658
C125	0.33502	0.95459	0.503

C126	0.50153	0.8766	0.43178
C127	0.34402	0.95389	0.22004
H128	0.91592	0.83904	0.99654
O129	0.79363	0.72627	0.71657
N130	0.37371	0.90884	0.39103
O131	0.98497	0.9193	0.28209
O132	0.81688	0.92474	0.31994
H133	0.35272	0.92413	0.6419
H134	0.50231	0.8175	0.36119
H135	0.238	0.93828	0.08459
C136	0.85647	0.79028	0.68774
H137	0.96675	0.84101	0.45755
H138	0.83341	0.78607	0.53094
H139	0.81667	0.84984	0.70369
H140	0.97036	0.78693	0.80518
C141	0.40093	0.37343	0.30708
C142	0.32199	0.31008	0.1468
C143	0.34129	0.29929	0.00192
C144	0.27105	0.2398	0.85658
C145	0.83502	0.45459	0.503
C146	0.00153	0.3766	0.43178
C147	0.84402	0.45389	0.22004
H148	0.41592	0.33904	0.99654
O149	0.29363	0.22627	0.71657
N150	0.87371	0.40884	0.39103
O151	0.48497	0.4193	0.28209
O152	0.31688	0.42474	0.31994
H153	0.85272	0.42413	0.6419
H154	0.00231	0.3175	0.36119
H155	0.738	0.43828	0.08459
C156	0.35647	0.29028	0.68774
H157	0.46675	0.34101	0.45755
H158	0.33341	0.28607	0.53094
H159	0.31667	0.34984	0.70369
H160	0.47036	0.28693	0.80518
Cu161	0.09667	0	0.47005
O162	0.21646	0	0.3866
H163	0.41791	0	0.18425
Cu164	0.59667	0.5	0.47005
O165	0.71646	0.5	0.3866
H166	0.91791	0.5	0.18425
Cu167	0.90333	0	0.52995
O168	0.78354	0	0.6134
H169	0.58209	0	0.81575

Cu170	0.40333	0.5	0.52995
O171	0.28354	0.5	0.6134
H172	0.08209	0.5	0.81575

Table S2. Comparison table with other reported MOFs for the detection of $Cr_2O_7^{2-}$ions.

Fluorescent material	Media	$K_{sv}(M^{-1})$	LOD(M)	Reference
Cu-OCH_3 MOF	H_2O	4.5935×10^3	6.27×10^{-6}	This work
MOF-801	H_2O	-	3×10^{-5}	1
Cd-MOF	EtOH	9.429×10^4	4.96×10^{-6}	2
Cd-MOF(IV)	H_2O	4.68×10^3	2.47×10^{-6}	3
QDs@UiO-66-NH_2	H_2O	3.12×10^4	1.6×10^{-4}	4
Yb-MOF	DMF	5.99×10^3	1.24×10^{-6}	5
Ln-MOFs	H_2O	3.012×10^3	2.9×10^{-6}	6
JLNU-10-Tb	H_2O	1.37×10^4	1.54×10^{-6}	7
Zn-MOF	H_2O	1.966×10^4	2.56×10^{-5}	8
CUST-983	DCM	1.2916×10^5	4.81×10^{-7}	9
CUST-851	EtOH	2.1×10^4	1.33×10^{-4}	10
$Tb_{0.5}Y_{0.5}$-MOF	H_2O	6.532×10^3	0.26×10^{-6}	11
Zn-MOF	H_2O	7.40×10^5	3.71×10^{-6}	12
Zn-MOF	H_2O	2.17×10^4	4×10^{-4}	13
Cd-MOF	H_2O	1.23×10^3	6.9×10^{-5}	14
Zn-MOF	H_2O	1.023×10^6	1.7×10^{-8}	15
Cd-MOF	H_2O	9.077×10^4	5.949×10^{-8}	16
Cd-MOF	H_2O	2.746×10^4	2.9×10^{-7}	17
Ln-MOF	DMF	7.661×10^5	1.7409×10^{-8}	18
Eu(III)-MOF	H_2O	3.3×10^4	2.59×10^{-9}	19
Hf-BITD	H_2O	9.5×10^4	3.3×10^{-10}	20

References

1. J. Yoo, U. Ryu, W. Kwon and K. M. Choi, A multi-dye containing MOF for the ratiometric detection and simultaneous removal of $Cr_2O_7^{2-}$ in the presence of interfering ions, *Sens. Actuators B Chem.*, 2019, **283**, 426-433.
2. Q. Wen, J.-L. Chen, J.-F. Song, S.-Y. Zhou, H.-Y. Zhu and X.-Q. Zhang, Synthesis of novel coordination polymer Cd-MOF and fluorescent probe detection of Fe^{3+}, $Cr_2O_7^{2-}$, and ceftriaxone sodium (CRO), *J. Mol. Struct.*, 2024, **1300**, 137235-137245.
3. H.-y. Yang, Z.-z. Chen, D.-y. Qi, Y.-j. Deng, Z.-x. Liu, M.-y. Cao, C.-y. Shao and L.-r. Yang, One cadmium (II)-based metal–organic framework as high-efficiency multi-functional fluorescence chemosensor targeting for the determination of Fe^{3+}, $Cr_2O_7^{2-}$ and CrO_4^{2-} in aqueous phase, *J. Alloys Compd.*, 2021, **876**, 160115-160128.
4. K.-N. Chi, Y. Guan, X. Zhang, T. Yang, S. Meng, R. Hu and Y.-H. Yang, Iodide/metal-organic frameworks (MOF) -mediated signal amplification strategy for the colorimetric detection of H_2O_2, $Cr_2O_7^{2-}$ and H_2S, *Anal. Chim. Acta.*, 2021, **1159**, 338378-338387.
5. Y. Zhang, J. Liu, X. Wu, W. Tao and Z. Li, Ultrasensitive detection of Cr(VI) ($Cr_2O_7^{2-}$/CrO_4^{2-}) ions in water environment with a fluorescent sensor based on metal-organic frameworks combined with sulfur quantum dots, *Anal. Chim. Acta.*, 2020, **1131**, 68-79.
6. H. Yang, D. Qi, L. Guo, N. Fan, C. Shao, W. Zhang and L. Yang, A multifunctional luminescent chemosensor of YbIII-MOF for the detection of Nitrobenzene, Fe^{3+} and $Cr_2O_7^{2-}$, *Colloids Surf. A Physicochem. Eng. Asp.*, 2022, **633**, 127851-127860.
7. S.-R. Zhang, W.-T. Zhang, X. Li, G.-J. Xu, W. Xie, Y.-H. Xu, N. Xu and Z.-M. Su, Multifunctional Lanthanide Metal–Organic Frameworks Act as Fluorescent Probes for the Detection of $C_{r2}O_7^{2-}$, Fe^{3+}, and TNP, White Light-Emitting Diodes, and Luminescence Thermometers, *Inorg. Chem.*, 2025, **64**, 2990-2999.
8. T.-T. Li, Y.-H. Mo and S.-R. Zheng, An ultramicroporous Zn(II)-MOF with an open tubular channel for the gas adsorption and luminescent sensing of $Cr_2O_7^{2-}$, *J. Mol. Struct.*, 2026, **1350**, 144023-144030.
9. X. Wang, X. Li, Y. Wang, W. Zhang, X. Wang and Z.-m. Su, Designable Fluorescent Anthracene-Based Cd-Metal–Organic Frameworks for Sensing TNP, Fe^{3+}, and $Cr_2O_7^{2-}$, *Cryst. Growth Des.*, 2025, **25**, 3404-3413.
10. T. Zhen, X. Xiao, C.-H. Wang, X.-S. Wu, Y.-Q. Gu, T. Su, X. Han, Y. Cao and Z.-M. Su, Dual-Functional Viologen-Based Metal–Organic Framework for Thermochromic and Fluorescence Detection of Fe^{3+}, $Cr_2O_7^{2-}$, and Tetracycline, *Inorg. Chem.*, 2025, **64**, 16336-16346.
11. Z. Hu, Q. Deng, Z. Jiang, Z. Guo and D. Guo, "AIE+ESIPT" bis Schiff-base ligands with multicolor emission and their corresponding Eu(III) complexes: Synthesis and properties research, *J. Lumin.*, 2020, **220**, 116929-116939.
12. R. Dai, Y. Song, X. Ma, Z. Kong and X. Chen, Design and synthesis of a novel Zn(II) coordination compound for the highly selective detection of $Cr_2O_7^{2-}$, Cu^{2+}, Co^{2+}, and Ni^{2+}, *J. Mol. Struct.*, 2026, **1359**, 145284-145296.
13. S.-W. Dong, L.-N. Zheng, S. Liu, Y.-Z. Sun, N. Xue, J. Zhao and T. Ding, Novel highly stable zinc(II)-MOF based on metal-/carbonate-/5-ATZ- orientation for CO_2/CH_4 and C_2H_2/CO_2 gas adsorption separation and fluorescence detection of Fe^{3+}/Cr^{6+}, *J. Mol. Struct.* , 2026, **1350**, 144036-144045.
14. H.-M. Yan, H. Chen, Y.-L. Wu, C.-K. Jiao and Y.-T. Yan, A Cd(II)-based Metal-Organic Frameworks (MOFs) with new topological net as multi-functional chemical sensor in detecting Fe^{3+}, CrO_4^{2-} and $Cr_2O_7^{2-}$, *J. Solid State Chem.*, 2025, **345**, 125211-125218.

15. V. Hubale, A. Dalvi, O. Nille, G. Kolekar and V. Sawant, Zn(II)/Cd(II) MOFs as multifunctional fluorescent sensors for sensitive detection of Al^{3+}, $Cr_2O_7^{2-}$ and glucose, *J. Mol. Struct.* , 2026, **1356**, 145089-145102.
16. Y. Cao, K.-X. Yuan and Y. Wang, "Turn-off" Cd-MOF fluorescence sensor for identification and detection of Fe^{3+}, Cr^{6+} and antibiotics in aqueous solutions, *Dyes Pigm.* , 2025, **242**, 112999-113010.
17. B. B. Xiong, T. C. Yue, X. Y. Yao, L. L. Wang and D. Z. Wang, Two New Luminescent Metal–Organic Frameworks as Fluorescent Sensors of Nitrobenzene, Fe^{3+}, and $Cr_2O_7^{2-}$, *Appl. Organomet. Chem.*, 2024, **39**, e7866-e7875.
18. J. Li, S. Zhang, L. Fan, Y. Yang and R. Wen, A Novel Multifunctional Eu (III) - MOF Luminescence Sensor for Detecting NB, Fe^{3+}, and $Cr_2O_7^{2-}$ With Outstanding Sensitivities and Selectivities, *Appl. Organomet. Chem.*, 2024, **39**, e7887-e7896.
19. W. Liu, Y. Wang, Z. Bai, Y. Li, Y. Wang, L. Chen, L. Xu, J. Diwu, Z. Chai and S. Wang, Hydrolytically Stable Luminescent Cationic Metal Organic Framework for Highly Sensitive and Selective Sensing of Chromate Anions in Natural Water Systems, *ACS Appl. Mater. Interfaces.*, 2017, **9**, 16448-16457.
20. X. Wang, Z.-J. Li, Y. Ju, X. Li, J. Qian, M.-Y. He, J.-Q. Wang, Z.-H. Zhang and J. Lin, A MOF-based luminometric sensor for ultra-sensitive and highly selective detection of chromium oxyanions, *Talanta*, 2023, **252**, 123894-123901.